

Silicalite nanoparticles that promote transgene expression

Megan E Pearce¹, Hoang Q Mai¹, Namhoon Lee²,
Sarah C Larsen^{2,3} and Aliasger K Salem^{1,3}

¹ Division of Pharmaceutics, College of Pharmacy, University of Iowa, Iowa City, IA 52242, USA

² Department of Chemistry, College of Liberal Arts and Sciences, University of Iowa, Iowa City, IA 52242, USA

E-mail: sarah-larsen@uiowa.edu and aliasger-salem@uiowa.edu

Received 22 January 2008, in final form 26 February 2008

Published 25 March 2008

Online at stacks.iop.org/Nano/19/175103

Abstract

Here, we report on a new zeolite-based silicalite nanoparticle that can enhance the transfection efficiencies generated by poly ethylene imine–plasmid DNA (PEI–pDNA) complexes via a sedimentation mechanism and can enhance the transfection efficiencies of pDNA alone when surface functionalized with amine groups. The silicalite nanoparticles have a mean size of 55 nm. Functionalizing the silicalite nanoparticles with amine groups results in a clear transition in zeta potential from -25.9 ± 2.3 mV (pH 7.4) for unfunctionalized silicalite nanoparticles to 4.9 ± 0.7 mV (pH 7.4) for amine functionalized silicalite nanoparticles. We identify that silicalite nanoparticles used to promote non-viral vector acceleration to the cell surface are found in acidic vesicles or the cytoplasm but not the nucleus. An MTT (3-[4,5-dimethylthiazol-2-yl]-2,5-diphenyl tetrazolium bromide) assay showed that the silicalite nanoparticles were non-toxic at the concentrations tested for transfection. We show that surface functionalization of silicalite nanoparticles with amine groups results in a significant (230%) increase in transfection efficiency of pDNA when compared to unfunctionalized silicalite nanoparticles. Silicalite nanoparticles enhanced pDNA–PEI induced transfection of human embryonic kidney (HEK-293) cells by over 150%.

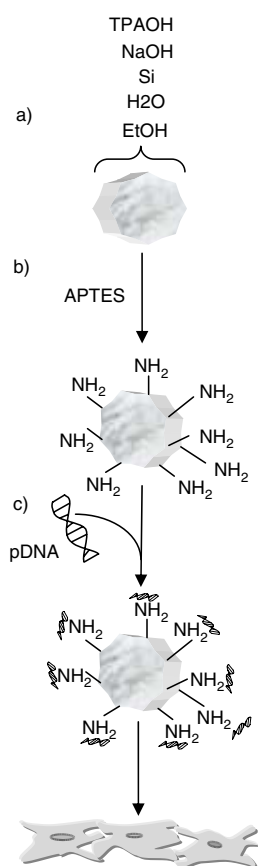
There is a critical need to enhance the transgene expression of gene delivery systems for research and clinical applications [1]. Gene delivery can be achieved using viral or non-viral vectors [2]. Viral vectors have substantially higher transfection efficiencies than non-viral vectors but are difficult and time-consuming to prepare and have poor storage stability in comparison to non-viral vectors. In addition, several safety concerns with respect to viral vectors still remain [2]. Non-viral vectors have been prepared from a wide variety of materials ranging from liposomes to cationic polymers [1, 3]. However, the transfection efficiencies of most of the non-viral vectors still fall far below those of their viral counterparts [4]. In recent years, inorganic silica nanoparticles have shown significant potential for enhancing the transfection efficiencies of plasmid DNA (pDNA) *in vitro* and *in vivo* [5–7]. For example, silica particles surface functionalized with amino groups and electrostatically bound with pDNA generated high

levels of transfection in neuronal-like cells with no observation of toxicity after four weeks [7]. Silica nanoparticles are biologically inert, have very low toxicity and are amenable to surface functionalization with a wide variety of molecules and functional groups [8–11]. The use of silica nanoparticles in non-viral gene delivery has broadly fallen into two categories. The first is the use of silica nanoparticles to enhance the concentration of pDNA vectors at the cell surface [12–14]. This is a sedimentation-based mechanism in which the nanoparticle mass is used to counteract the viscosity of the incubation medium [14]. The increased concentration of pDNA at the cell surface mediated by this improved sedimentation rate is reported to substantially enhance the transfection efficiencies [14]. The silica nanoparticles used in these studies did not contribute to any toxicity observed by the commercially available Superfect vector [13]. However, silica nanoparticles without a transfection reagent did not enhance gene expression [14]. In contrast, several other groups have

³ Authors to whom any correspondence should be addressed.

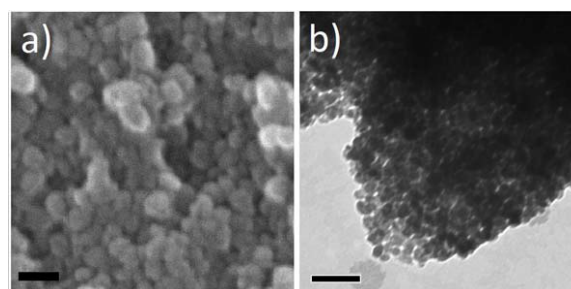
Table 1. Classification, functionalization, size, shape and zeta potential of the silicalite nanoparticles. The zeta potential measurements are expressed as mean \pm standard deviation and are representative of at least three repeats.

Sample	Functionalization	Mean size/shape	Zeta potential (mV)
Silicalite	None	55 nm, spherical irregular	-25.9 ± 2.3
Silicalite-amine	$-\text{NH}_2$	55 nm, spherical irregular	4.9 ± 0.7

**Figure 1.** Schematic showing the preparation of the amine functionalized silicalite nanoparticles. (a) The silicalite nanoparticles are synthesized as described in the text. (b) The silicalite nanoparticles are surface functionalized using APTES. (c) Plasmid DNA (pDNA) or PEI-pDNA polyplexes (not shown) are mixed with the silicalite nanoparticles and incubated with the HEK-293 cells for 4 h.

shown that silica nanoparticles have significant potential as non-viral vectors that are directly responsible for delivery of the pDNA [7, 15, 6]. In these cases, the silica nanoparticles have been functionalized with surface amine groups [7, 15]. The cationic nanoparticles can bind electrostatically to the phosphate backbone of pDNA, condensing it and thereby protecting the pDNA from enzymatic degradation and promoting delivery into cells [5].

Here, we report on a new zeolite-based silicalite nanoparticle that can enhance the transfection efficiencies generated by poly ethylene imine-plasmid DNA (PEI-pDNA) complexes via a sedimentation mechanism and can enhance the transfection efficiencies of pDNA alone when surface

**Figure 2.** (a) An SEM micrograph showing the surface morphology of the silicalite nanoparticles. (b) A TEM micrograph showing the shape of the same particles. The size bars are 0.15 μm and 0.3 μm , respectively.

functionalized with amine groups. We show, for the first time, that surface functionalization of silicalite nanoparticles with amine groups significantly promotes the transfection of pDNA alone but not PEI-pDNA complexes when compared to unfunctionalized silicalite nanoparticles. We also identify the cellular fate of silicalite nanoparticles used to promote non-viral vector acceleration to the cell surface.

In this study, we selected silicalite-1 nanoparticles as a novel candidate for promoting the cell surface accumulation of pDNA. Silicalite-1 is an all-silica zeolite with an MFI-type framework which consists of elliptical pores ($\sim 5.6 \text{ \AA}$) [16]. Nanocrystalline zeolites are biocompatible, crystalline hydrated aluminosilicates (or silicates) with crystal sizes of 100 nm or less [17–19]. Zeolites have well-defined channels and cavities of molecular dimensions and anionic frameworks which are charge-compensated with alkaline or alkaline earth metals [17].

Figure 1 shows our general approach to preparation of functionalized silicalite nanoparticles. Silicalite-1 nanocrystals with a mean approximate size of 55 nm were synthesized from a clear solution that was composed of 9TPAOH: 0.16NaOH: 25Si: 495H₂O: 100EtOH, where TPAOH is tetrapropylammonium hydroxide [17]. The clear solution was refluxed at 60 °C for 240 h, washed and centrifuged. X-ray diffraction verified the formation of the silicalite-1 phase. Scanning electron microscopy (SEM) and transmission electron microscopy (TEM) images showed that the silicalite nanoparticles had smooth surfaces with irregular spherical shapes (table 1, figures 2(a) and (b)). To functionalize the silicalite nanoparticles, samples (55 nm silicalite calcined at 500 °C in air) were mixed with 3-aminopropyltriethoxysilane (APTES) in 60 ml of toluene in a round-bottom flask [20, 21]. The sample was heated in an oil bath for 4 h at 120 °C. The resulting solution was filtered to separate the functionalized

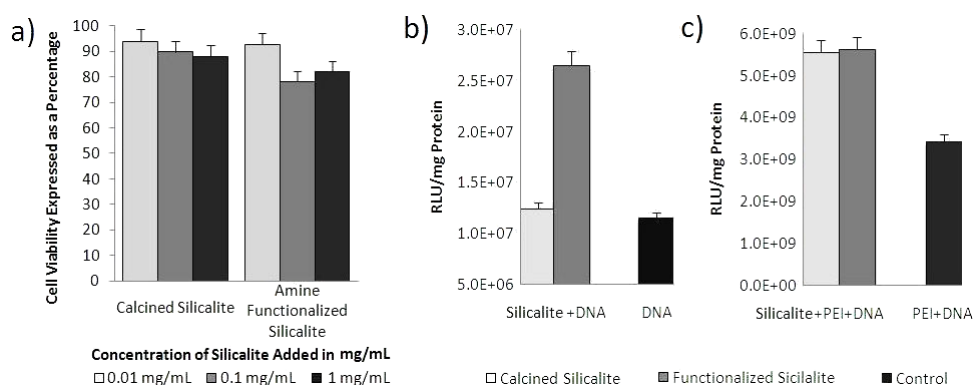


Figure 3. (a) MTT toxicity assay results for unfunctionalized and amine functionalized silicalite nanoparticles at three different concentrations: 0.01, 0.1 and 1 mg ml⁻¹. Transfection results for the (b) unfunctionalized and amine functionalized silicalite nanoparticles with pDNA only and (c) unfunctionalized and amine functionalized silicalite nanoparticles with pDNA-PEI polyplexes. The results are presented as mean \pm standard deviation and are representative of at least three repeats.

silicalite nanoparticles from the solution. Confirmation of the functionalization of the silicalite nanoparticles was observed by a clear transition in zeta potential from -25.9 ± 2.3 mV (pH 7.4) for unfunctionalized silicalite nanoparticles to 4.9 ± 0.7 mV (pH 7.4) for amine functionalized silicalite nanoparticles. The particle properties are summarized in table 1. The size and shape of the silicalite nanoparticles did not significantly change following functionalization.

To determine the degree of pDNA bound to the amine functionalized silicalite nanoparticles, pDNA encoding 6.4 kb firefly luciferase (pCMV-luciferase VR122_C) driven by the cytomegalovirus (CMV) promoter/enhancer was mixed with functionalized silicalite nanoparticles at pH 5.7. The surface pDNA concentration was determined using absorbance spectroscopy. Functionalized silicalite nanoparticles bound 14.1 ± 2.3 μ g pDNA per mg silicalite nanoparticles. In contrast, non-functionalized silicalite nanoparticles demonstrated much lower pDNA binding of 3.6 ± 0.6 μ g pDNA per mg silicalite nanoparticles. These results are consistent with previous studies that have shown that post synthetic modification of the silica surface with aminopropyl groups can increase the maximum DNA adsorption to 15.7 μ g mg⁻¹ silica [22]. Also consistent with previous studies, high salt and alkaline pH hinder pDNA binding with the functionalized silicalite nanoparticles [5]. These results confirm that functionalized silicalite nanoparticles bind with pDNA electrostatically and that the binding interaction is dependent on protonation of the amine functionalized silicalite nanoparticles.

Our target dose of silicalite nanoparticle promoters in the transfection experiments was 0.01 mg ml⁻¹. This dose was significantly below the LD50 value (the dose lethal to 50% of the cells). Analysis of the toxicity was determined using the 3-(4,5-dimethylthiazol-2-yl)-2,5-diphenyltetrazolium bromide (MTT) assay (figure 3(a)). Even at dosing levels 1000-fold higher than our target dose, the LD50 value was not reached. The decreases in cell viability were proportional to the silicalite nanoparticle dose, but qualitative microscopic analysis showed that, at the higher concentrations, this was not due to adverse particle interaction following internalization by the cells but rather the high concentration of silicalite nanoparticles forming

a blanket over the cell monolayer that was presumably causing cell-membrane damage and/or preventing diffusion of nutrients from the medium to the cells. Previous studies using the lactate dehydrogenase assay have shown that low to medium concentrations of silica nanoparticles are non-toxic but high concentrations of silica nanoparticles can induce cell-membrane damage [23]. Amine functionalization of the silicalite nanoparticles did not significantly increase the toxicity in comparison to unfunctionalized silicalite nanoparticles ($P > 0.05$).

Next, we tested six groups for transfection efficiency in a model HEK-293 cell line that is widely utilized for testing non-viral vectors. The six groups included (1) amine functionalized silicalite nanoparticles with pDNA, (2) amine functionalized silicalite nanoparticles with pDNA-PEI polyplexes, (3) non-functionalized silicalite nanoparticles with pDNA, (4) non-functionalized silicalite nanoparticles with pDNA-PEI polyplexes, (5) pDNA-PEI polyplexes alone, and (6) pDNA alone. Plasmid DNA-PEI polyplexes were prepared at an N:P ratio of 5:1 and had a zeta potential of +15 to +20 mV and sizes ranging from 150 to 400 nm.

Figure 3(b) shows that amine functionalized silicalite nanoparticles increased the transfection efficiency of pDNA by 230% ($P < 0.05$). In comparison, non-functionalized silicalite nanoparticles resulted in no significant increase in transfection efficiency in comparison to naked pDNA ($P > 0.05$). These results were consistent with pDNA binding studies. In contrast, both unfunctionalized and functionalized silicalite nanoparticles enhanced the pDNA-PEI induced transfection of HEK-293 cells by over 150% ($P < 0.05$). PEI is a cationic polymer that is widely utilized for *in vitro* non-viral gene delivery. The positive charge of the PEI results in effective electrostatic binding to the negatively charged pDNA, and this condensation protects the pDNA from digestion in serum and as the complex enters cells. Once in the endosomal compartment, PEI can act as a buffer or 'proton sponge' to induce osmotic swelling and cause release from the endosome, which results in enhanced transfection efficiencies [4]. Silicalite nanoparticles are therefore primarily promoting the transfection of PEI-

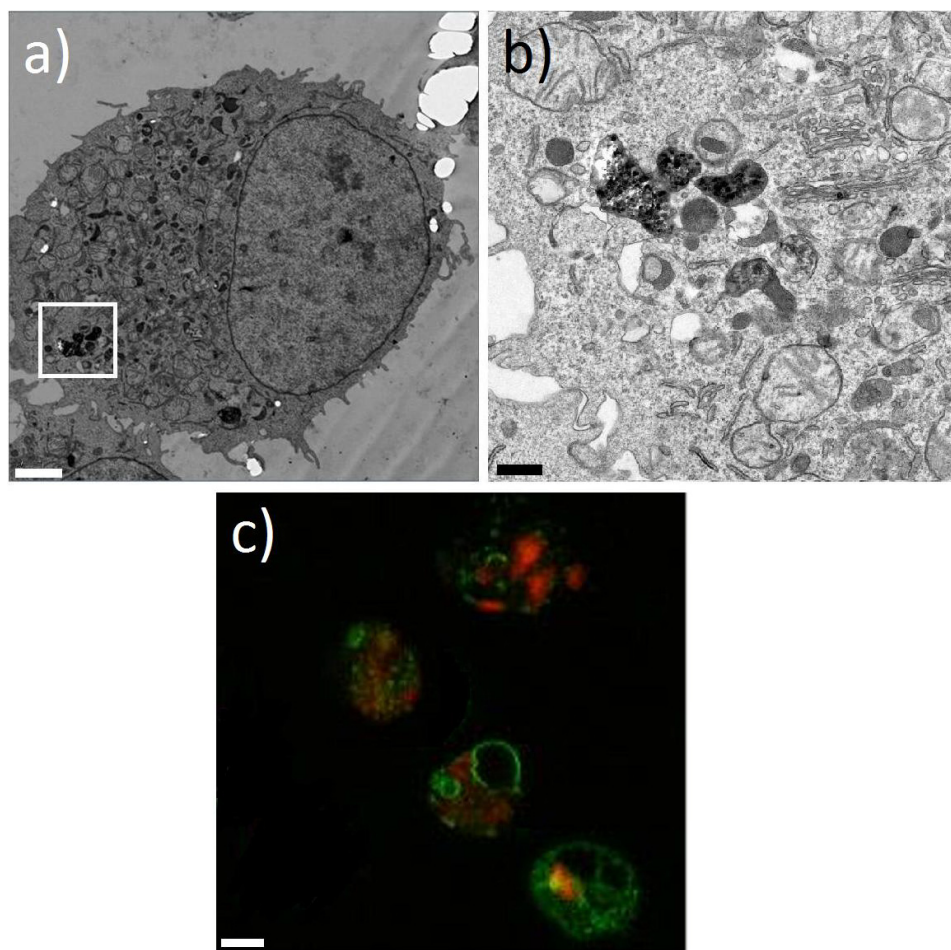


Figure 4. (a) A representative TEM image of an HEK-293 cell showing vesicle entrapped and cytoplasmic distribution of amine functionalized silicalite particles. (b) A magnification (white box) of the silicalite nanoparticles within the same cell from (a). (c) A confocal image containing some examples of functionalized silicalite nanoparticles within the membranes of the cells. The nanoparticles are red (rhodamine stained, 633 nm) whilst the cells have their acidic organelles stained green (lysotracker green stained, 543 nm). The size bars are 0.2 μm , 0.5 μm , and 10 μm , respectively.

pDNA polyplexes by increasing the concentration of PEI-pDNA polyplexes at the cell surface.

Several studies have shown the cellular fate of PEI-pDNA polyplexes once they enter the cell [24, 25]. Silica nanoparticles tracked using fluorescent microscopy have been observed to be internalized by the endosomal-lysosomal pathway followed by perinuclear accumulation [12]. To determine the cellular fate of the silicalite nanoparticles used to sediment the PEI-pDNA polyplexes and the pDNA alone in our studies, we used TEM and confocal microscopy analysis. Figures 4(a) and (b) show a representative TEM section of silicalite nanoparticles within the HEK-293 cell. Silicalite nanoparticles could be found within vesicles or the cytoplasm but never the nucleus. Inhibition of endocytosis has been reported to reduce transfection efficiencies by up to 3000%, indicating the importance of this uptake mechanism [14]. Unfunctionalized and amine functionalized silicalite nanoparticles promoting sedimentation of pDNA and PEI-pDNA polyplexes to the cell surface are clearly internalized into the cells. However, they are not responsible for chaperoning the pDNA to the nucleus. These results

were confirmed by incubating rhodamine labeled silicalite nanoparticles with cells stained with lysotracker green. Confocal microscopy images after 24 h (figure 4(c)) showed that, consistent with the TEM analysis, silicalite nanoparticles were present in the cytoplasm or the acidic organelles but not the nucleus. In future studies, given the endocytic mechanism of uptake, chloroquine, an endosomolytic agent could be used to promote the release of the silicalite nanoparticles from the endosomes into the cytoplasm to further increase the transfection efficiencies of pDNA alone [15, 26].

In summary, we have shown that novel zeolite-based silicalite nanoparticles can be readily functionalized with amine groups that promote the transfection efficiency of pDNA. Surface functionalization with amine groups can impart a positive charge on the silicalite nanoparticles but does not significantly change the size, shape or toxicity. We have shown that silicalite nanoparticles are non-toxic promoters for the transfection efficiency induced by PEI-pDNA polyplexes but that amine functionalization of the silicalite nanoparticles does not promote or reduce this transfection efficiency further. Finally, we show that silicalite nanoparticles promote

accumulation and internalization of pDNA and PEI-pDNA polyplexes in HEK-293 cells but do not chaperone the pDNA to the nucleus. Silicalite nanoparticles are an adaptable low-cost material capable of undergoing a variety of physical and chemical modifications and should find widespread utility in promoting pDNA-based transfection of cells [20, 18].

1. Methods and materials

1.1. Cell culture

Human embryonic kidney (HEK-293) cells were obtained from the American Type Culture Collection (ATCC, Rockville, MD). The cells were maintained in Dulbecco's modified eagle's medium (DMEM) supplemented with 10% fetal bovine serum (FBS), streptomycin at 100 $\mu\text{g ml}^{-1}$, penicillin at 100 U ml^{-1} , and 4 mM L-glutamine at 37 °C in a humidified 5% CO₂-containing atmosphere.

1.2. Amplification and purification of plasmid DNA (pDNA)

VR1255 plasmid is a 6.4 kb cDNA encoding firefly luciferase driven by the cytomegalovirus (CMV) promoter/enhancer. The pDNA was transformed in *Escherichia coli* DH5 α and amplified in Terrific Broth media at 37 °C overnight with a shaking speed of 300 rpm. The pDNA was purified by an endotoxin-free QIAGEN Giga plasmid purification kit (QIAGEN, Valencia, CA) according to the manufacturer's protocol. Purified pDNA was dissolved in saline, and its purity and concentration were determined by UV absorbance at 260 and 280 nm.

1.3. Particle size and zeta potential analysis

Nanoparticle size measurements were conducted using the Zetasizer Nano ZS (Malvern, Southborough, MA). Briefly, the nanoparticles were suspended in an aqueous medium at a concentration of 1 mg ml^{-1} . The size measurements were performed at 25 °C at a 173° scattering angle. The mean hydrodynamic diameter was determined by cumulative analysis. The zeta potential determinations were based on electrophoretic mobility of the nanoparticles in the aqueous medium, which were performed using folded capillary cells in automatic mode.

1.4. Scanning electron microscope (SEM) imaging

The nanoparticle morphology was assessed by scanning electron microscopy (SEM, Hitachi S-4000). Briefly, air-dried nanoparticles were placed on adhesive carbon tabs mounted on SEM specimen stubs. The specimen stubs were coated with approximately 5 nm of gold by ion beam evaporation before examination in the microscope, operated at 5 kV accelerating voltage.

1.5. Plasmid DNA binding analysis

Plasmid DNA was incubated with amine functionalized silicalite nanoparticles and unfunctionalized silicalite nanoparticles in PBS (pH adjusted to 6.4) at concentrations varying from

1 $\mu\text{g pDNA mg}^{-1}$ particle to 90 $\mu\text{g pDNA mg}^{-1}$ particle. The mixture was allowed to incubate at 4 °C for 24 h. The resulting nanoparticles were centrifuged at 13 200 rpm for 5 min on an Eppendorf microcentrifuge in order to ensure that all nanoparticles were removed from solution. The supernatant was collected and analyzed spectrophotometrically at 260 nm using a SpectraMax Plus³⁸⁴ microplate spectrophotometer (Molecular Devices, Sunnyvale, CA) for pDNA content. The amount of plasmid DNA bound to the silicalite nanoparticles was calculated by subtracting the pDNA content in the supernatant from the initial concentration of pDNA added. All measurements were repeated at least three times.

1.6. Toxicity studies

The toxicity analysis was completed using the MTT assay. HEK-293 cells were seeded in a 96-well plate at a density of 10 000 cells per well. After 24 h, they were incubated with 200 μl of complete DMEM containing nanoparticles or nanoparticle-pDNA complexes at a concentration of 0.01, 0.1 or 1.0 mg ml^{-1} . After 4 h of incubation, the medium in each well was replaced with 100 μl of fresh complete medium. 25 μl of 5 mg ml^{-1} MTT solution in PBS was added to each well and incubated with the cells for an additional 2 h. The cells were lysed with 100 μl of the extraction buffer (20% SDS in 50% DMF, pH 4.7) overnight. The optical density of the lysate was measured at 550 nm using a Spectramax plus³⁸⁴ microplate spectrophotometer. Values were expressed as a percentage of the control to which nothing was added, and were representative of at least three repeats.

1.7. Transfection experiments

HEK-293 cells were seeded into 24-well plates at a density of 8×10^4 well^{-1} 24 h before transfection. Amine functionalized silicalite nanoparticles and unfunctionalized silicalite nanoparticles were prepared in individual batches of 0.01 mg ml^{-1} in purified and 0.2 μm filtered water. Plasmid DNA (VR1255) was first mixed with PEI (high molecular weight, water free; Sigma Aldrich, St Louis, MO) at an N:P ratio of 5:1, briefly vortexed and allowed to sit for 25 min at room temperature. After 25 min, the PEI-pDNA polyplexes (1 $\mu\text{g pDNA}$) or pDNA (1 μg) were incubated with 20 μl of the silicalite nanoparticle solution for another 8 min. Finally, the silicalite nanoparticles and/or polyplexes/pDNA were added to the cells in Opti-MEM transfection medium (serum-free) and incubated for 4 h at 37 °C. This was followed by incubation in serum containing medium for 44 h.

The cells were then treated with 200 μl of lysis buffer (Promega, Madison, WI). The lysate was subjected to two cycles of freezing and thawing, then transferred into tubes and centrifuged. 20 μl of supernatant was added to 100 μl of luciferase assay reagent (Promega, Madison, WI) and samples were measured on a luminometer for 10 s (Lumat LB 9507, EG&G Berthold, Bad Wildbad, Germany). The relative light units (RLUs) were normalized against protein content using a BCA protein assay kit (Pierce, Rockford, IL). Luciferase activity was expressed as relative light units (RLU/mg protein in the cell lysate).

1.8. Transmission electron microscope (TEM) imaging

For TEM analysis, HEK-293 cells were seeded into a 12-well plate at a density of 8×10^4 /well 24 h before silicalite nanoparticles were introduced. Amine functionalized silicalite nanoparticles and unfunctionalized silicalite nanoparticles with and without pDNA or PEI-pDNA polyplexes were prepared in individual batches of 0.01 mg ml^{-1} in purified and $0.2 \mu\text{m}$ filtered water. Approximately $20 \mu\text{l}$ of each 0.01 mg ml^{-1} solution was added to the cells. The particles were allowed to incubate for 24 h. Following incubation, the cells were fixed in aldehyde solution. After a short incubation in the fixative, the wells were rinsed twice with buffer followed by incubation in a 1% OsO_4 buffer (4% osmium/6% potassium ferrocyanide). Subsequent brief washings were completed in the following order: 2.5% uranyl acetate, 25% ethanol, 50% ethanol, 75% ethanol, 95% ethanol and 100% ethanol. Two eponate incubations followed these washings. The resulting liquid was incubated in the wells overnight, and this was followed by 90 nm slicing using a Leica UC6 ultramicrotome. The samples were mounted on carbon-coated 100-mesh copper grids and then stained with 4% uranyl acetate. Imaging was on a JEOL JEM-1230 transmission electron microscope.

1.9. Confocal microscope imaging

Confocal microscopy studies of nanoparticle uptake in cells were carried out using a similar protocol to the TEM studies. Prior to adding the silicalite nanoparticles to the cells, however, they were first functionalized with a rhodamine fluorescent label using N-hydroxysuccinimide chemistry (Molecular Probes, Eugene, OR). The solutions were washed, reconstituted in complete DMEM and covered to prevent bleaching of the dye prior to imaging.

For the silicalite nanoparticle uptake studies, HEK-293 cells were seeded on four 4-well cover slips at $8 \times 10^4 \text{ ml}^{-1}$ 24 h before silicalite nanoparticle incubation with or without pDNA or PEI-pDNA polyplexes. Approximately $20 \mu\text{l}$ of each 0.01 mg ml^{-1} solution was added to the cells. The silicalite nanoparticles were allowed to incubate for 24 h. Following incubation, the complete media was aspirated and replaced with lysotracker green (Molecular Probes, Eugene, OR) in complete DMEM at a concentration of $50 \times 10^{-9} \text{ M}$. The lysotracker medium was replaced after one hour with regular complete DMEM medium, after which the samples were allowed to rest for one further hour. Imaging was completed on a Bio-Rad Radiance 2100MP multiphoton/confocal microscope.

1.10. Statistical analysis

Group data were reported as mean \pm SD. Differences between groups were analyzed by one-way analysis of variance with a Tukey post-test analysis. Levels of significance were accepted at the $P < 0.05$ level. Statistical analyses were performed using Prism 3.02 software (Graphpad Software, Inc., San Diego, CA).

Acknowledgments

A K Salem and S C Larsen acknowledge grant support from NSF NER (CMMI-0608977). H Q Mai and N Lee acknowledge support from the Iowa Biosciences Advantage Program. The authors thank H Arul for assistance in the preparation of silicalite-APTES samples.

References

- [1] Luo D and Saltzman W M 2000 Synthetic DNA delivery systems *Nat. Biotechnol.* **18** 33–7
- [2] Kataoka K and Harashima H 2001 Gene delivery systems: viral versus non-viral vectors *Adv. Drug Deliv. Rev.* **52** 151
- [3] Zhang X Q, Intra J and Salem A K 2007 Conjugation of polyamidoamine dendrimers on biodegradable microparticles for non-viral gene delivery *Bioconjug. Chem.* **6** 2068–76
- [4] Abbas A O, Donovan M D and Salem A K 2007 Formulating PLGA particles for plasmid DNA delivery *J. Pharm. Sci.* at press doi:10.1002/jps.21215
- [5] Kneuer C, Sameti M, Haltner E G, Schiestel T, Schirra H, Schmidt H and Lehr C M 2000 Silica nanoparticles modified with aminosilanes as carriers for plasmid DNA *Int. J. Pharm.* **196** 257–61
- [6] Radu D R, Lai C Y, Jeftinija K, Rowe E W, Jeftinija S and Lin V S Y 2004 A polyamidoamine dendrimer-capped mesoporous silica nanosphere-based gene transfection reagent *J. Am. Chem. Soc.* **126** 13216–7
- [7] Bharali D J, Klejbor I, Stachowiak E K, Dutta P, Roy I, Kaur N, Bergey E J, Prasad P N and Stachowiak M K 2005 Organically modified silica nanoparticles: a nonviral vector for *in vivo* gene delivery and expression in the brain *Proc. Natl Acad. Sci. USA* **102** 11539–44
- [8] Slowing II, Trewyn B G, Giri S and Lin V S Y 2007 Mesoporous silica nanoparticles for drug delivery and biosensing applications *Adv. Funct. Mater.* **17** 1225–36
- [9] Torney F, Trewyn B G, Lin V S Y and Wang K 2007 Mesoporous silica nanoparticles deliver DNA and chemicals into plants *Nat. Nanotechnol.* **2** 295–300
- [10] Santra S, Liesenfeld B, Dutta D, Chatel D, Batich C D, Tan W H, Moudgil B M and Mericle R A 2005 Folate conjugated fluorescent silica nanoparticles for labeling neoplastic cells *J. Nanosci. Nanotechnol.* **5** 899–904
- [11] Slowing I, Trewyn B G and Lin V S Y 2006 Effect of surface functionalization of MCM-41-type mesoporous silica nanoparticles on the endocytosis by human cancer cells *J. Am. Chem. Soc.* **128** 14792–3
- [12] Gemeinhart R A, Luo D and Saltzman W M 2005 Cellular fate of a modular DNA delivery system mediated by silica nanoparticles *Biotechnol. Prog.* **21** 532–7
- [13] Luo D, Han E, Belcheva N and Saltzman W M 2004 A self-assembled, modular DNA delivery system mediated by silica nanoparticles *J. Control. Release* **95** 333–41
- [14] Luo D and Saltzman W M 2000 Enhancement of transfection by physical concentration of DNA at the cell surface *Nat. Biotechnol.* **18** 893–5
- [15] Kneuer C, Sameti M, Bakowsky U, Schiestel T, Schirra H, Schmidt H and Lehr C M 2000 A nonviral DNA delivery system based on surface modified silica-nanoparticles can efficiently transfect cells *in vitro* *Bioconjug. Chem.* **11** 926–32
- [16] Kumar S, Davis T M, Ramanan H, Penn R L and Tsapatsis M 2007 Aggregative growth of silicalite-1 *J. Phys. Chem. B* **111** 3398–403
- [17] Song W, Justice R E, Jones C A, Grassian V H and Larsen S C 2004 Size-dependent properties of nanocrystalline silicalite synthesized with systematically varied crystal sizes *Langmuir* **20** 4696–702

- [18] Song W, Kanthasamy R, Grassian V and Larsen S 2004 Hexagonal, hollow, aluminium-containing ZSM-5 tubes prepared from mesoporous silica templates *Chem. Commun.* **17** 1920–1
- [19] Zampieri A, Mabande G T P, Selvam T, Schwieger W, Rudolph A, Hermann R, Sieber H and Greil P 2006 Biotemplating of *Luffa cylindrica* sponges to self-supporting hierarchical zeolite macrostructures for bio-inspired structured catalytic reactors *Mater. Sci. Eng. C* **26** 130–5
- [20] Song W, Woodworth J F, Grassian V H and Larsen S C 2005 Microscopic and macroscopic characterization of organosilane-functionalized nanocrystalline NaZSM-5 *Langmuir* **21** 7009–14
- [21] Zhan B Z, White M A and Lumsden M 2003 Bonding of organic amino, vinyl, and acryl groups to nanometer-sized NaX zeolite crystal surfaces *Langmuir* **19** 4205–10
- [22] Solberg S M and Landry C C 2006 Adsorption of DNA into mesoporous silica *J. Phys. Chem. B* **110** 15261–8
- [23] Chang J S, Chang K L B, Hwang D F and Kong Z L 2007 *In vitro* cytotoxicity of silica nanoparticles at high concentrations strongly depends on the metabolic activity type of the cell line *Environ. Sci. Technol.* **41** 2064–8
- [24] Suh J, Wirtz D and Hanes J 2003 Efficient active transport of gene nanocarriers to the cell nucleus *Proc. Natl Acad. Sci. USA* **100** 3878–82
- [25] Godbey W T, Wu K K and Mikos A G 1999 Tracking the intracellular path of poly(ethylenimine)/DNA complexes for gene delivery *Proc. Natl Acad. Sci. USA* **96** 5177–81
- [26] Salem A K, Searson P C and Leong K W 2003 Multifunctional nanorods for gene delivery *Nat. Mater.* **2** 668–71